International Journal of Minerals, Metallurgy and Materials
Volume 23, Number 9, September 2016, Page 1112
DOI: 10.1007/s12613-016-1329-6

Synthesis and characterization of Fe_3O_4@SiO_2 magnetic composite nanoparticles by a one-pot process

Le Zhang, Hui-ping Shao, Hang Zheng, Tao Lin, and Zhi-meng Guo

Institute for Advanced Materials and Technology, University of Science and Technology Beijing, Beijing 100083, China

(Received: 26 October 2015; revised: 18 May 2016; accepted: 20 May 2016)

Abstract: Fe_3O_4@SiO_2 core–shell composite nanoparticles were successfully prepared by a one-pot process. Tetraethyl–orthosilicate was used as a surfactant to synthesize Fe_3O_4@SiO_2 core–shell structures from prepared Fe_3O_4 nanoparticles. The properties of the Fe_3O_4 and Fe_3O_4@SiO_2 composite nanoparticles were studied by X-ray diffraction, transmission electron microscopy, energy dispersive spectroscopy, and Fourier transform infrared spectroscopy. The prepared Fe_3O_4 particles were approximately 12 nm in size, and the thickness of the SiO_2 coating was approximately 4 nm. The magnetic properties were studied by vibrating sample magnetometry. The results show that the maximum saturation magnetization of the Fe_3O_4@SiO_2 powder (34.85 $A{\cdot}m^2{\cdot}kg^{-1}$) was markedly lower than that of the Fe_3O_4 powder (79.55 $A{\cdot}m^2{\cdot}kg^{-1}$), which demonstrates that Fe_3O_4 was successfully wrapped by SiO_2. The Fe_3O_4@SiO_2 composite nanoparticles have broad prospects in biomedical applications; thus, our next study will apply them in magnetic resonance imaging.

Keywords: composite materials; magnetite nanoparticles; iron oxides; silicon dioxide; one-pot process

1. Introduction

Magnetic fluid comprises magnetic nanoparticles, a surfactant, and a carrier liquid. The magnetic nanoparticles, which are the main component, are modified by the surfactant, which not only reduces their agglomeration and uneven dispersion but also endows them with good compatibility. In addition, the application of a magnetic fluid is determined by the carrier liquid [1]. Paramagnetic iron oxide nanoparticles have promising application prospects as bio-magnetic materials, because they possess the advantages of both paramagnetism and properties originating from the nanoscale effect. Furthermore, these nanoparticles are non-toxic and thus stable *in vivo* [2]. Water-based magnetic fluid containing Fe_3O_4 nanoparticles has broad potential applications as a magnetic resonance imaging (MRI) contrast agent [3] and in the removal of heavy metal ions from aqueous solution [4], biological cell separation [5], targeted drug delivery [6], and magnetic hyperthermia and catalysis [7]. However, Fe_3O_4 nanoparticles aggregate easily due to the nanoscale effect and magnetic gravitational effect [8]. SiO_2 nanoparticles have good hydrophilicity, stability, and biocompatibility, which effectively improve the performance of Fe_3O_4 nanoparticles in biological applications [9] and allow the attachment of organic molecules to the nanoparticle surface by covalent bonds. Wrapping the surface of Fe_3O_4 nanoparticles with SiO_2 to form Fe_3O_4@SiO_2 core–shell nanoparticles is an effective means of preventing the agglomeration of these nanoparticles.

Fe_3O_4@SiO_2 composite nanoparticles have the desirable properties of magnetic nanoparticles while also benefiting from the SiO_2 shell. The hydroxyl functional groups of SiO_2 facilitate the ornamentation, grafting, and joining of these nanoparticles with drug carriers, which is beneficial for their application in MRI research [10]. Fe_3O_4@SiO_2@chitosan or glucan magnetic composite nanoparticles exhibit good magnetism, hydrophilicity, stability, and biocompatibility, thereby improving the image quality of MRI. When these nanoparticles are injected into biological systems under an external magnetic field, different magnetic relaxation time are produced, enhancing the MRI resolution ratio. In addition, these magnetic composite nanoparticles are non-toxic and can be excreted in urine, making them promising MRI contrast agents [11–12].

Corresponding author: Hui-ping Shao E-mail: shaohp@ustb.edu.cn

Fe_3O_4@SiO_2 composite nanoparticles have been prepared by the micro-emulsion method and Stöber hydrolysis method, as reported in many previous studies [13]. In this study, Fe_3O_4@SiO_2 was prepared by a one-pot process, which differs from the conventional two-step approach in which Fe_3O_4 nanoparticles are prepared in the first step and then used as seeds for the growth of silica in the second step. The composite nanoparticles were characterized by X-ray diffraction (XRD), transmission electron microscopy (TEM), energy-dispersive X-ray spectroscopy (EDS), Fourier transform infrared spectroscopy (FTIR), and vibrating sample magnetometry (VSM) at room temperature. The results show that this one-pot synthesis is a low-cost and convenient method for the preparation of Fe_3O_4@SiO_2 core–shell nanoparticles. Moreover, the results of this work will provide the foundation for our next study in which these nanoparticles are applied as MRI contrast agents.

2. Experimental

2.1. Chemicals

Ferric chloride hexahydrate ($FeCl_3 \cdot 6H_2O$), ferrous sulfate heptahydrate ($FeSO_4 \cdot 7H_2O$), ammonia hydroxide ($NH_3 \cdot H_2O$), tetraethyl orthosilicate (TEOS), and sodium dodecyl benzene sulfonate (SDBS) were purchased from China National Pharmaceutical Group Chemical Reagent Co., Ltd. Ethanol was purchased from Beijing Chemical Industry Group Co. All chemicals mentioned above were of analytical purity. Deionized water was used in all experiments.

2.2. Synthesis of Fe_3O_4@SiO_2 magnetic composite nanoparticles

Referring to a previously published procedure [14–16], 15 mL of deionized water in a 250-mL beaker was heated in a water bath to 75°C, at which point 0.81 g of $FeCl_3 \cdot 6H_2O$ and 0.556 g of $FeSO_4 \cdot 7H_2O$ were added to the beaker. Next, 3 mL of ammonia was added quickly, and the reaction was conducted for 25 min at 75°C. SDBS (0.12 g) was then added as a surface modifier to reduce the agglomeration of the Fe_3O_4 nanoparticles, and the reaction was continued for 50 min at 75°C under stirring. The solution was then separated into two equal batches. The first batch (marked as S1) was washed with deionized water and ethanol alternately, providing the Fe_3O_4 nanoparticles used as a basis of comparison for the composite nanoparticles. The second batch (marked as S2) was dispersed in 96 mL of deionized water by an ultrasonicator for 30 min at room temperature. The solution was then transferred to a 1000-mL beaker, after which 480 mL of ethanol was added and mixed uniformly, 15 mL of ammonia was added slowly, and then 4.8 mL of TEOS (as Fig. 1(b)) was added. The reaction was conducted for 8 h at room temperature and stirring at 300 r/min. Finally, the Fe_3O_4@SiO_2 magnetic composite nanoparticles were obtained.

Fig. 1 shows the TEM images of the Fe_3O_4@SiO_2 core–shell composite nanoparticles prepared with different amounts of TEOS: 3.6 mL, 4.8 mL, and 6.0 mL. When 3.6 mL of TEOS was added, the Fe_3O_4@SiO_2 magnetic composite nanoparticle solution was cloudy. Meanwhile, when 6.0 mL of TEOS was added, the SiO_2 coating was too thick, degrading the quality of the prepared Fe_3O_4@SiO_2 composite nanoparticles and making them unsuitable for biological applications. However, when 4.8 mL of TEOS was added, the Fe_3O_4 nanoparticles were effectively wrapped by the SiO_2. Thus, 4.8 mL of TEOS was appropriate for this synthesis [17–18].

2.3. Characterization of Fe_3O_4 nanoparticles (S1) and Fe_3O_4@SiO_2 composite nanoparticles (S2)

The Fe_3O_4 nanoparticles (S1) and Fe_3O_4@SiO_2 composite nanoparticles (S2) were characterized by XRD, TEM, EDS, FTIR, and VSM.

3. Results and discussion

3.1. X-ray diffraction analysis

Fig. 2 shows the XRD patterns of the Fe_3O_4 nanoparticles and Fe_3O_4@SiO_2 composite nanoparticles. As shown in Fig. 2, the position and intensity of the Fe_3O_4 diffraction peak (the S1 curve) were consistent with the powder diffraction file (PDF) standard card. Peaks were detected at 2θ = 30.1°, 35.4°, 43.0°, 53.4°, 56.9°, and 62.6°, corresponding to the (220), (311), (400), (422), (511), and (440) crystal planes, respectively [19]. According to the Scherrer formula, $D = K \cdot \lambda / (\beta \cdot \cos\theta)$ (θ: diffraction angle; K: Scherrer constant, K = 0.89; λ = 0.154 nm; β: diffraction peak half-width) [18], the Fe_3O_4 nanoparticles were 12 nm in size. A broad peak was observed at 2θ = 20°~24.3° in the S2 curve, which may correspond to the amorphous SiO_2 [20]. However, the absence of the three strong peaks characteristic of SiO_2 in this region made it impossible to prove this assignment. Thus, more work must be performed to confirm whether the Fe_3O_4 nanoparticles were coated by SiO_2 nanoparticles. The shapes and locations of the other peaks in S2 clearly corresponded to Fe_3O_4 nanoparticles, revealing that the structures of the Fe_3O_4 nanoparticles were not changed in S2. Therefore, according to the XRD patterns of the magnetic composite nanoparticles, Fe_3O_4 may have been coated by SiO_2.

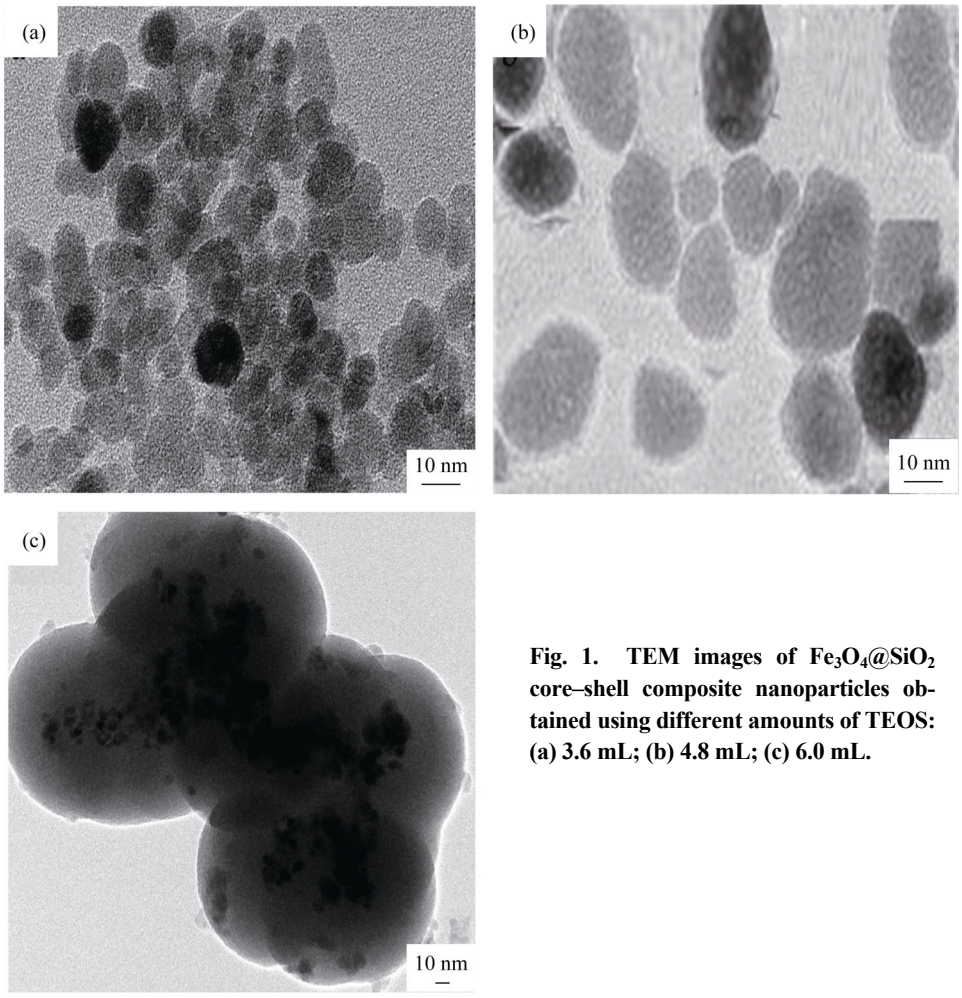

Fig. 1. TEM images of Fe_3O_4@SiO_2 core–shell composite nanoparticles obtained using different amounts of TEOS: (a) 3.6 mL; (b) 4.8 mL; (c) 6.0 mL.

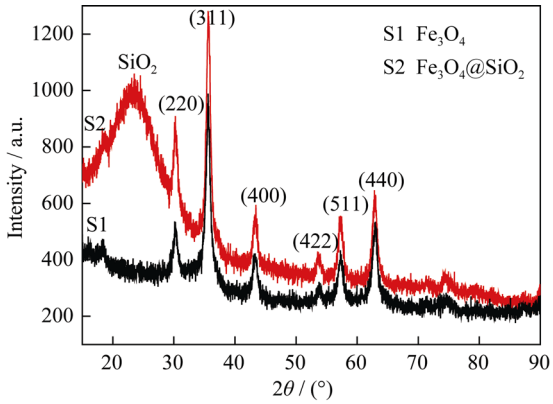

Fig. 2. XRD patterns of Fe_3O_4 nanoparticles and Fe_3O_4@SiO_2 composite nanoparticles.

3.2. Transmission electron microscopy study

TEM images of the Fe_3O_4 nanoparticles and Fe_3O_4@SiO_2 core–shell composite nanoparticles are shown in Fig. 3. As evident in Fig. 3(a), the Fe_3O_4 nanoparticles were spherical, regular in shape, and uniform in size. The Fe_3O_4 nanoparticles were found to be approximately 12 nm in size, which was consistent with the results from the Scherrer equation based on the XRD data. Comparing Figs. 3(a)–(c), it is obvious that the Fe_3O_4 particles were coated with SiO_2, as verified by the EDS and FTIR analyses described in subsequent sections. In the high-resolution TEM image of the Fe_3O_4@SiO_2 composite nanoparticles presented in Fig. 3(c), it is clear that the surface of the Fe_3O_4 nanoparticles was coated by SiO_2.

3.3. Energy-dispersive X-ray analysis

The EDS analysis of the Fe_3O_4 nanoparticles (S1) and Fe_3O_4@SiO_2 composite nanoparticles (S2) are presented in Fig. 4. Peaks corresponding to Fe, O, C, and Si are observed in both the S1 and S2 curves, whereas a strong Si peak is observed markedly in S2. According to Table 1, the compositions of Si and Fe (by weight) were 1.40% and 28.10%, respectively, for the Fe_3O_4 nanoparticles, but 23.6% and 10.20%, respectively, for the Fe_3O_4@SiO_2 composite nanoparticles; this difference provides further evidence that

the Fe_3O_4 surface was coated with SiO_2 [21]. The high-resolution TEM image of the Fe_3O_4@SiO_2 composite nanoparticles as well as the FTIR and VSM data indicate that the SiO_2 layer was located on the surface of the Fe_3O_4 nanoparticles, not that the SiO_2 was physically mixed with the Fe_3O_4 nanoparticles.

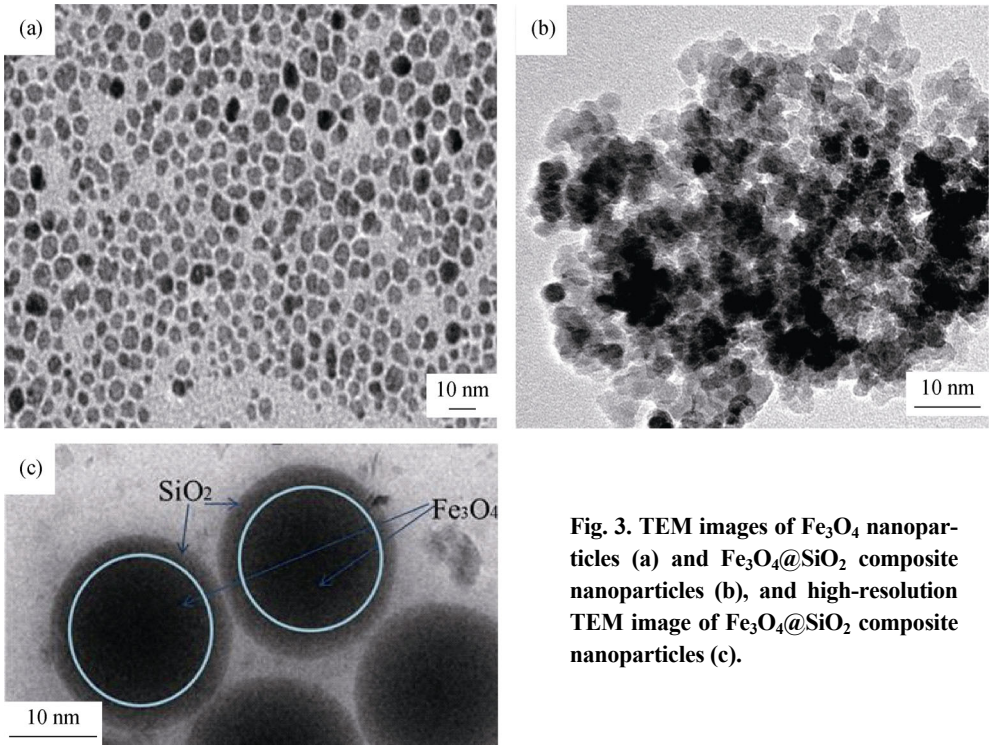

Fig. 3. TEM images of Fe_3O_4 nanoparticles (a) and Fe_3O_4@SiO_2 composite nanoparticles (b), and high-resolution TEM image of Fe_3O_4@SiO_2 composite nanoparticles (c).

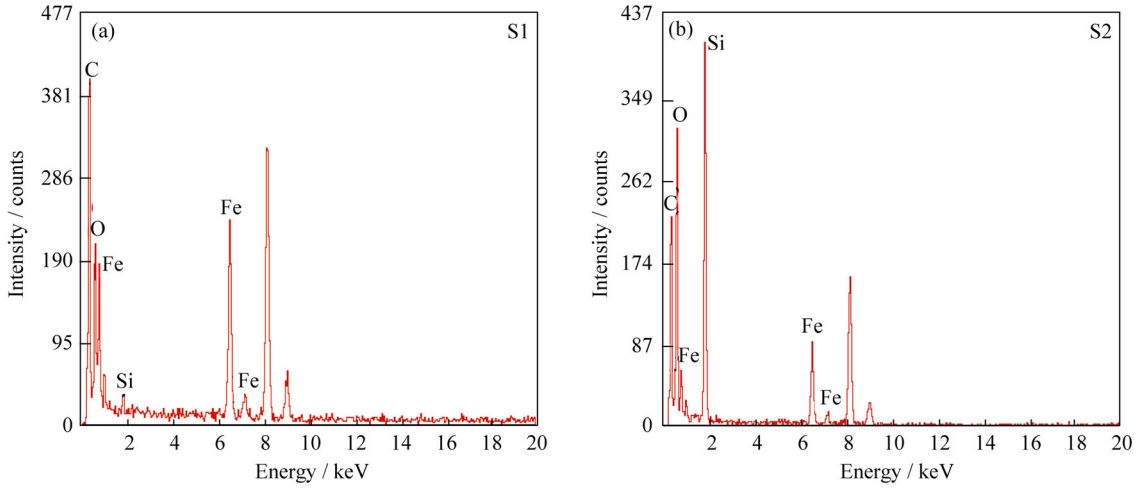

Fig. 4. EDS spectra of Fe_3O_4 nanoparticles (S1) and Fe_3O_4@SiO_2 composite nanoparticles (S2).

Table 1. Elemental compositions of Fe_3O_4 nanoparticles (S1) and Fe_3O_4@SiO_2 composite nanoparticles (S2) identified by EDS.

Element	Mass fraction / %		Atom fraction / %	
	S1	S2	S1	S2
C K	51.80	39.20	71.40	46.80
O K	18.70	33.30	19.40	35.60
Si K	01.40	23.60	00.80	14.40
Fe K	28.10	10.20	08.40	03.10

3.4. Fourier transform infrared spectroscopy study

The FTIR spectra of Fe_3O_4 nanoparticles (S1) and Fe_3O_4@SiO_2 composite nanoparticles (S2) are compared in Fig. 5. These spectra show that a thin SiO_2 layer was present on the surface of the Fe_3O_4 and that this SiO_2 was generated from TEOS to form Fe–O–Si bonds [22–23]. The two curves featured a peak at approximately 3424 cm^{-1}, which was due to O–H stretching vibrations [24], and small peaks at approximately 2361 cm^{-1}, which were due to C–H bending vibrations. The peak at approximately 1624 cm^{-1} was due to H–O–H bending vibrations [25], while the peak at 565 cm^{-1} was due to Fe–O stretching vibrations [26]. In the spectrum for S2, the peaks at approximately 1091 cm^{-1} and 799 cm^{-1} were due to Si–O–Si symmetric and asymmetric stretching vibrations, respectively, whereas the peak at approximately 950 cm^{-1} was due to Si–O stretching vibrations [27]. Therefore, based on these FTIR data, it was concluded that SiO_2 was present in the composite nanoparticles and that the Fe_3O_4 was successfully wrapped by SiO_2 [28].

3.5. Magnetic properties of the composite nanoparticles

Photographs of S1 (Fe_3O_4 aqueous solution) and S2 (Fe_3O_4@SiO_2 composite aqueous solution) are shown in Fig. 6(a), while the photographs of Fe_3O_4 aqueous solution and Fe_3O_4@SiO_2 composite aqueous solution approached by a magnet are shown in Fig. 6(b). Fig. 6(a) shows that the Fe_3O_4 nanoparticles and Fe_3O_4@SiO_2 composite nanoparticles exhibited good dispersibility in an aqueous medium and that the former was black, but the latter was brown. When the solution was approached by a magnet, the magnetic nanoparticles were attracted (as Fig. 6(b)), rapidly turning the water solution clear [29].

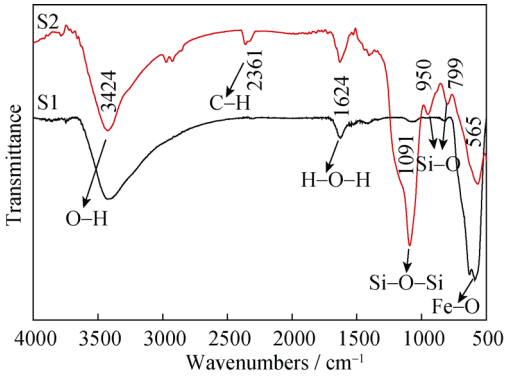

Fig. 5. FTIR spectra of Fe_3O_4 nanoparticles (S1) and Fe_3O_4@SiO_2 composite nanoparticles (S2).

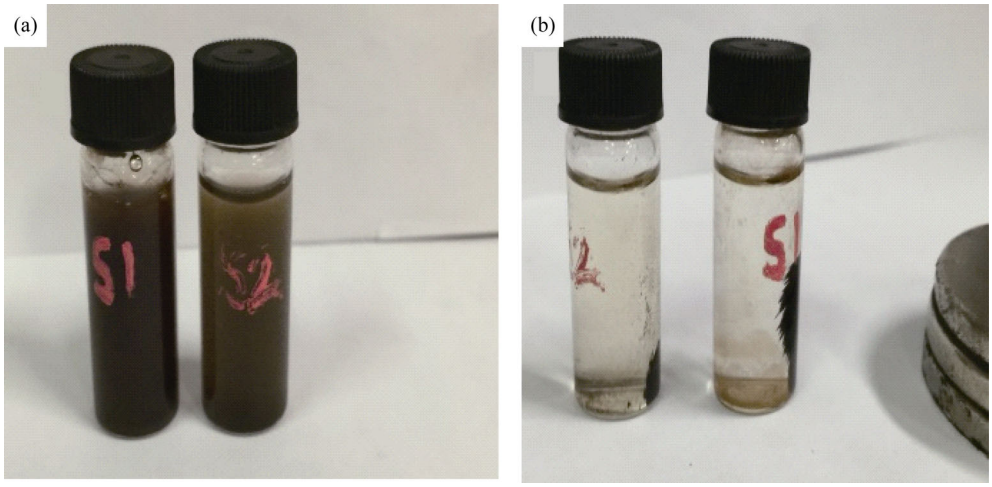

Fig. 6. Photographs of the aqueous nanoparticle solutions: (a) approached by nothing; (b) approached by a magnet.

The magnetic properties of the Fe_3O_4 nanoparticles (S1) and Fe_3O_4@SiO_2 composite nanoparticles (S2) were measured at room temperature by VSM as the magnetic field varied from –20.0 kOe to 20.0 kOe, as shown in Fig. 7. The saturation magnetizations of the Fe_3O_4 nanoparticles and Fe_3O_4@SiO_2 composite nanoparticles were 79.55 $A{\cdot}m^2{\cdot}kg^{-1}$ and 34.85 $A{\cdot}m^2{\cdot}kg^{-1}$, respectively; the lower value for the composite nanoparticles was due to the reduction of the Fe_3O_4 relative content by coating with SiO_2.

The Fe_3O_4 nanoparticles (S1) and Fe_3O_4@SiO_2 composite nanoparticles (S2) demonstrated paramagnetic properties. As the external magnetic field strength increased, the magnetization first increased rapidly and then reached saturation. Then, as the external magnetic field strength decreased, the magnetization of the sample returned along the original route, showing S-type behavior and nearly no residual magnetism and coercivity force, which is significant for biomedical applications. However, the Fe_3O_4 nanoparticles (S1) and Fe_3O_4@SiO_2 composite nanoparticles demonstrated very weak residual magnetism and coercivity in Fig. 8. As

presented in Table 2, the Fe_3O_4 nanoparticles and Fe_3O_4@SiO_2 composite nanoparticles had residual magnetisms of 2.297 $A·m^2·kg^{-1}$ and 1.667 $A·m^2·kg^{-1}$, respectively, and coercive forces of 22 Oe and 18 Oe, respectively. The coercivities of all samples were less than 100 Oe; therefore, they would be considered paramagnetic in biological applications [30]. In our next study, the Fe_3O_4@SiO_2 composite nanoparticles will be coated with chitosan or glucan to be used as an MRI contrast agent, enhancing the resolution ratio of MRI.

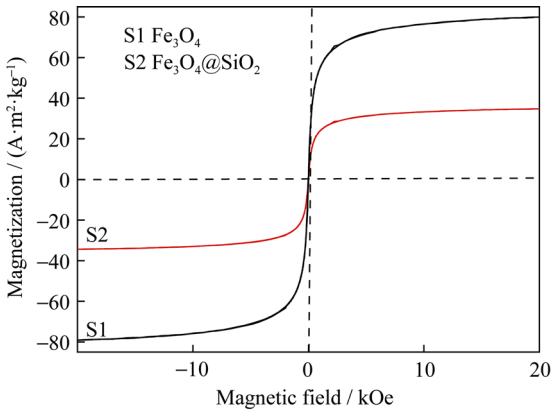

Fig. 7. Magnetic curves of Fe_3O_4 nanoparticles and Fe_3O_4@SiO_2 composite nanoparticles.

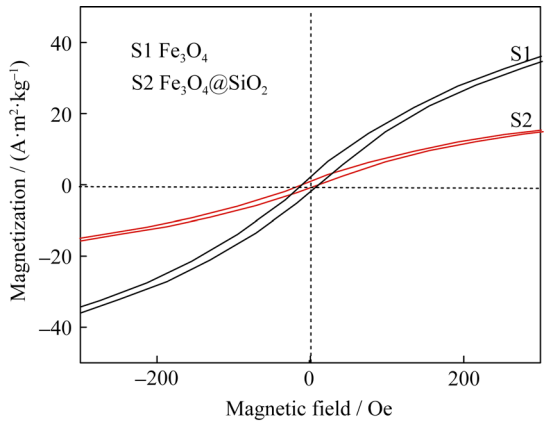

Fig. 8. Enlarged view of VSM results for Fe_3O_4 nanoparticles and Fe_3O_4@SiO_2 composite nanoparticles.

Table 2. Magnetic properties of Fe_3O_4 nanoparticles and Fe_3O_4@SiO_2 composite nanoparticles.

Material	Saturation magnetization / ($A·m^2·kg^{-1}$)	Residual magnetization / ($A·m^2·kg^{-1}$)	Coercivity / Oe
Fe_3O_4	79.55	2.297	22
Fe_3O_4@SiO_2	34.85	1.667	18

4. Conclusions

(1) Fe_3O_4@SiO_2 core–shell magnetic composite nanoparticles were prepared successfully by a cost-effective one-pot process. The Fe_3O_4 magnetic particles were approximately 12 nm in size, and the SiO_2 coating was approximately 4 nm thick. Based on the TEM results, the Fe_3O_4 was spherical, regular in shape, and uniform in size, and the SiO_2 coating layer was uniform. The results showed that the Fe_3O_4 core was coated by SiO_2 particles.

(2) The saturation magnetization of the Fe_3O_4 nanoparticles was 79.55 $A·m^2·kg^{-1}$, while that of the Fe_3O_4@SiO_2 composite nanoparticles was 34.85 $A·m^2·kg^{-1}$. This difference could be attributed to the SiO_2 coated layer.

(3) Although the magnetism of the Fe_3O_4@SiO_2 composite nanoparticles was lower than that of the Fe_3O_4 nanoparticles, it still satisfied the requirements for biological applications. This work laid the foundation for our next study, which will apply these composite nanoparticles to MRI contrast agents.

Acknowledgements

We gratefully acknowledge the National Natural Science Foundation of China (No. 51274039), the State Key Lab of Advanced Metals and Materials (No. 2013-ZD05) and the Guangdong Foundation of Research (No. 2014B090901003).

References

[1] L. Kang, P. Hu, J. Yang, H. Wang, F. Yang, J. J. Du, and Z. L. Yang, Applications of magnetic Fe_3O_4 nanoparticles in biomedical field, *Mater. Rev.*, 29(2015), No. 11, p. 132.

[2] J.Y. Wu, Q. Xu, Z. Li, Z.Q. Li, and X. Huang, Preparation and properties of magnetic silica nanoparticles, *J. Wuhan Inst. Technol.*, 36(2014), No. 7, p. 43.

[3] B.K. Sodipo and A.A. Aziz, Non-seeded synthesis and characterization of superparamagnetic iron oxide nanoparticles incorporated into silica nanoparticles via ultrasound, *Ultrason. Sonochem.*, 23(2015), p. 354.

[4] G.Z. Li, M. Liu, Z.Q. Zhang, C. Geng, Z.B. Wu, and X. Zhao, Extraction of methylmercury and ethylmercury from aqueous solution using surface sulfhydryl-functionalized magnetic mesoporous silica nanoparticles, *J. Colloid. Interface Sci.*, 424(2014), p. 124.

[5] M. Arvand and M. Hassannezhad, Magnetic core–shell Fe_3O_4@SiO_2/MWCNT nanocomposite modified carbon paste electrode for amplified electrochemical sensing of uric acid, *Mater. Sci. Eng. C.*, 36(2014), p. 160.

[6] M. Sedlák, D.S. Bhosale, L. Beneš, J. Palarčík, A. Kalendová, K. Královec, and A. Imramovský, Synthesis and characterization of a pH-sensitive conjugate of isoniazid with Fe_3O_4@SiO_2 magnetic nanoparticles, *Bioorg. Med. Chem. Lett.*, 23(2013), No. 16, p. 4692.

[7] M. Abbas, B.P. Rao, S.M. Naga, M. Takahashi, and C.G. Kim, Synthesis of high magnetization hydrophilic magnetite (Fe_3O_4) nanoparticles in single reaction: surfactantless polyol process, *Ceram. Int.*, 39(2013), p. 7605.

[8] L. Jiang, F. Gao, R. He, and D.X. Cui, Preparation and characterization of silica-coated Fe_3O_4 Nanoparticles, *J. Mater. Sci. Eng.*, 27(2009), No. 3, p. 352.

[9] H. Yan, J.C. Zhang, C.X. You, Z.W. Song, B.W. Yu, and Y. Shen, Surface modification of Fe_3O_4 nanoparticles and their magnetic properties, *Int. J. Miner. Metall. Mater.*, 16(2009), No. 2, p. 226.

[10] X. Bai, *Preparation and Characterization of Magnetic Mesoporous Silica Nanoparticles* (*Fe_3O_4@SiO_2*) *with a Core–Shell Structure* [Dissertation], Harbin Institute of Technology, Harbin, 2012, p. 27.

[11] Z.Y. Ren, *Synthesis and Characterization of Macromolecular MRI Contrast Agents Based on Water-soluble Chitosan Derivatives* [Dissertation], East China normal university, Shanghai, 2012, p. 22.

[12] D.J. Yu, M.Z. Li, X.Z. Huang, W.H. Zhu, Y. Huang, Q. Zhang, and Q. Liu, Preparation of and study on magnetic resonance imaging performance of metal porphyrin modified by low molecular weight chitosan, *Spectrosc. Spectral Anal.*, 33(2013), No. 10, p. 2736.

[13] L. Li, Z. L. Mo, R. B. Guo, H. D. Liu, L. Qi, and Q. J. Wu, New progress of surface modification of the magnetic Fe_3O_4 particles in biomedicine applications, *J Funct. Mater.*, 47(2016), No. 4, p. 4028.

[14] Y. Ji, H.P. Shao, Z.M. Guo, T. Lin, and D.H. Yang, Preparation of Fe_3O_4 magnetic nanoparticles by ultrasonic emulsification and research of magnetic fluids with chitosan modification, *J. Univ. Sci. Technol. Beijing*, 33(2011), No. 6, p. 751.

[15] Y.M. Tan, H.P. Shao, Y. Ji, T. Lin, and Z.M. Guo, Preparation and research of stable Fe_3O_4 magnetic nanofluids in kerosene, *Powder Metall. Ind.*, 30(2012), No. 3, p. 163.

[16] H. Zheng, H.P. Shao, and Z.F. Zhao, Preparation and characterization of silicone-oil based γ-Fe_2O_3/Fe_3O_4 magnetic fluid, *J. Funct. Mater.*, 46(2015), No. 19, p. 19037.

[17] X.J. Deng, *Preparation and Adsorption Properties of Functional Composite Materials Based on Magnetic Nanoparticles* [Dissertation], Tianjin University, Tianjin, 2013, p. 15.

[18] B.J. Ding, W.M. Chen, L.W. Fan, Y.H. Zheng, D. Lv, and Z.X. Lu, Preparation and characterization of Fe_3O_4@SiO_2 magnetic catalyst support, *Inorg. Chem. Ind.*, 46(2014), No. 11, p. 62.

[19] S.C. Cao, Preparation and characterization of nanosilica, *Sensor World*, 8(2013), No. 9, p. 7.

[20] B.K. Sodipo and A.A. Aziz, An *in-situ* functionalization of decanethiol monolayer on thin silica coated superparamagnetic iron oxide nanoparticles synthesized by non-seeded process, *Adv. Mater. Res.*, 1024(2014), p. 300.

[21] Y.L. Tang, L. Song, S.L. Yu, N.Y. Gao, J. Zhang, H.C. Guo, and Y.L. Wang, Enhanced adsorption of humic acid on amine functionalized magnetic mesoporous composite microspheres, *Colloids Surf. A*, 406(2012), p. 61.

[22] F. Hosseini, A. Panahifar, M. Adeli, H. Amiri, A. Lascialfari, F. Orsini, M.R. Doschak, and M. Mahmoudi, Synthesis of pseudopolyrotaxanes-coated superparamagnetic iron oxide nanoparticles as new MRI contrast agent, *Colloids Surf. B*, 103(2013), p. 652.

[23] Y.F. Zhu, Y. Fang, and S. Kaskel, Folate-conjugated Fe_3O_4@SiO_2 hollow mesoporous spheres for targeted anticancer drug delivery, *J. Phys. Chem. C*, 114(2010), No. 39, p. 16382.

[24] L. Lai, Q. Xie, L.N. Chi, W. Gu, and D.Y. Wu, Adsorption of phosphate from water by easily separable Fe_3O_4@SiO_2 core/shell magnetic nanoparticles functionalized with hydrous lanthanum oxide, *J. Colloid. Interface Sci.*, 465(2016), p. 76.

[25] Z.H. Wang, H.J. Fan, and B. Shi, The preparation and characterization of magnetic polymer, *Leather Sci. Eng.*, 24(2014), No. 3, p. 23.

[26] I.A. Barbosa, P.C. de Sousa Filho, D.L. da Silva, F.B. Zanardi, L.D. Zanatta, A.J. de Oliveira, O.A. Serra, and Y. Lamamoto, Metalloporphyrins immobilized in Fe_3O_4@SiO_2 mesoporous submicrospheres: reusable biomimetic catalysts for hydrocarbon oxidation, *J. Colloid. Interface Sci.*, 469(2016), p. 296.

[27] M. Abbas, B.P. Rao, M.N. Islam, S.M. Naga, M. Takahashi, C. Kim, Highly stable-silica encapsulating magnetite nanoparticles (Fe_3O_4/SiO_2) synthesized using single surfactantless-polyol process, *Ceram. Int.*, 40(2014), No. 1, p. 1379. Ceramics International

[28] S. Vivekanandhan, M. Venkateswarlu, D. Carnahan, M. Misra, A.K. Mohanty, and N. Satyanarayana, Sol–gel mediated surface modification of nanocrystalline $NiFe_2O_4$ spinel powders with amorphous SiO_2, *Ceram. Int.*, 39(2013), No. 4, p. 4105.

[29] F. Dang, N. Enomoto, J. Hojo, and K. Enpuku, Sonochemical coating of magnetite nanoparticles with silica, *Ultrason. Sonochem.*, 17(2010), No. 1, p. 193.

[30] F. Tian, G.C. Chen, P.W. Yi, J.C. Zhang, A.G. Li, J. Zhang, L.R. Zheng, Z.W. Deng, Q. Shi, R. Peng, and Q.B. Wang, Fates of Fe_3O_4@SiO_2 nanoparticles in human mesenchymal stem cells assessed by synchrotron radiation-based techniques, *Biomaterials*, 35(2014), No. 24, p. 6412.